Journal of Catalysis **183,** 368–372 (1999)
Article ID jcat.1999.2409, available online at http://www.idealibrary.com on IDEAL®

Photocatalytic Activity of Rutile $Ti_{1-x}Sn_xO_2$ Solid Solutions

Jun Lin,* Jimmy C. Yu,*,[1] D. Lo,† and S. K. Lam†

*Department of Chemistry and †Department of Physics, The Chinese University of Hong Kong, Shatin, New Territories, Hong Kong

Received November 9, 1998; revised January 4, 1999; accepted January 6, 1999

Sn substitution for Ti in rutile TiO_2 has been found to increase the photoactivity of the rutile by up to 15 times for the oxidation of acetone. The activity increases with increasing Sn in $Ti_{1-x}Sn_xO_2$ solid solution, and it peaks at a tin content of 0.075. Contrary to expectations, ζ potential measurements show that the poor photocatalytic activity of pure rutile is not due to the lack of hydroxyl groups on its surface. Photoexcited transient decay data relate the poor activity to the fast electron–hole recombination in rutile TiO_2, and the addition of Sn to the rutile TiO_2 lattice can effectively slow down the recombination rate. Diffuse reflectance UV–vis spectra of the solid solutions reveal a blue shift, indicating an increase in the bandgap of the semiconductor. Based on these experimental results, we believe that the origin of the high photoactivity of $Ti_{1-x}Sn_xO_2$ is the increase in its oxidation–reduction potential resulting from elevation of the solid solution's bandgap.

Key Words: **photocatalytic activity; oxidation–reduction potential; rutile; titanium dioxide; tin oxide; solid solution.**

INTRODUCTION

In the past decade, metal oxide semiconductors such as TiO_2, ZnO_2, and WO_3 have attracted a great deal of attention in the areas of water, air, and wastewater treatment since they can catalytically decompose volatile organic compounds in liquid and gas phases under the illumination of UV light (1–5). However, among these metal oxide semiconductors, TiO_2 in anatase form has proven to be the most suitable for widespread environmental application due to its high photocatalytic activity and its stability with respect to photocorrosion and chemical corrosion (1, 6). Many studies (7–10) have focused on the photocatalytic process, mechanism, and kinetics of anatase TiO_2 for the oxidation and reduction of a variety of organic and inorganic compounds. Recently, quantum-sized anatase TiO_2 doped with transition metal (11–13) and titanium dioxide supported on an adsorbent (14, 15) have become active research goals. In contrast to anatase, little attention has been paid to rutile TiO_2. The reason for this is its very poor photoactivity as a photocatalyst. Tsai and Cheng (16) attributed the poor photoactivity of rutile TiO_2 to the smaller amount of hydroxyl groups on its surface, which results in a higher hole–electron recombination rate. Sclafani *et al.* (17) examined several commercial and homemade TiO_2 samples and found that the photocatalytic activity of rutile TiO_2 was influenced by its preparation methods. Maruska and Ghosh (18) believed that the higher photoactivity of anatase TiO_2 is due to its higher Fermi level compared with rutile TiO_2. However, further studies similar to those on anatase TiO_2 have seldom been performed on rutile TiO_2 in the field.

For the present study, we synthesized solid solutions of $Ti_{1-x}Sn_xO_2$ ($0.00 \leq x \leq 0.10$) in pure rutile form by using the citric acid complexing method and determined the photocatalytic degradation rate of acetone in air over the surface of the solid solutions. Finally, an explanation for the increase in the photocatalytic activity of the solid solution $Ti_{1-x}Sn_xO_2$ is proposed based on the results of polycrystalline X-ray diffraction, UV–vis diffuse reflectance, transient absorption decay spectra, and ζ potential measurements on the solid solutions.

EXPERIMENTAL

Synthesis of $Ti_{1-x}Sn_xO_2$ Solid Solutions

The precursors used for synthesis of the solid solutions were $TiCl_4$ (99.9% Aldrich), $SnCl_4$ (>97.5% BDH), citric acid (99.7% AnalaR), and 5% HCl aqueous solution. $Ti_{1-x}Sn_xO_2$ ($x = 0.00$, 0.025, 0.05, 0.075, and 0.10) solid solutions were prepared by the citric acid complexing method. $TiCl_4$ and $SnCl_4$ in the required stoichiometry were respectively added to a HCl aqueous solution under vigorous agitation; then citric acid was added to this solution, followed by sonication for 15 min and aging for 24 h. The solution was heated on a hot plate to thoroughly remove HCl and H_2O under constant stirring. Finally, the resultant precipitates were calcined in air at 710°C for 3 h.

Measurement of Photocatalytic Activity

The photocatalytic activity experiments on the solid solutions of $Ti_{1-x}Sn_xO_2$ for the oxidation of acetone in air were performed at ambient temperature using a 7000-ml reactor. The photocatalysts were prepared by coating an aqueous suspension of the solid solutions onto three dishes with diameters of 6.0 cm. The weight of the photocatalyst used

[1] To whom correspondence should be addressed. E-mail: jimyu@cuhk.edu.hk. Fax: (852) 2603–5057.

0021-9517/99 $30.00

for each experiment was kept at about 0.27 g. The solid solutions as photocatalysts were pretreated in an oven at 100°C for 2 h and then cooled to room temperature before use.

After the dishes coated with the solid solution catalysts were placed in the reactor, a small amount of acetone was injected into the reactor. The reactor was connected to a dryer containing $CaCl_2$ which was used for controlling the initial humidity in the reactor. The analysis of acetone, carbon dioxide, and water vapor concentration in the reactor was conducted with a Photoacoustic IR Multigas Monitor (INNOVA Air Tech Instruments Model 1312). The acetone vapor was allowed to reach adsorption equilibrium with the catalysts in the reactor prior to an experiment. The initial concentration of acetone after the adsorption equilibrium was 350 ppm, which remained constant until a 15-W 365-nm UV lamp (Cole–Parmer Instrument Co.) in the reactor was switched on. The initial concentration of water vapor was 1.20 ± 0.01 vol%, and the initial temperature was 25 ± 1°C.

During the photocatalytic reaction, a near 3 : 1 ratio of carbon dioxide produced to acetone destroyed was observed, and the acetone concentration decreased linearly with increase in UV illumination time. Each reaction was followed for 30 min. To express the photocatalytic activity of the solid solutions, we used the degradation rate constant in units of parts per million per minute.

Characterization of $Ti_{1-x}Sn_xO_2$ Solid Solutions

The polycrystalline X-ray diffraction patterns of the solid solutions were recorded with a Philips MPD 18801 diffractometer using Cu$K\alpha$ radiation, and single-crystal silicon was used as the standard to determine instrumental peak broadening. Diffuse reflectance UV–vis spectra of the powder solid solutions in the range 330–450 nm were obtained by using a Shimadzu UV–2501PC spectrometer with $BaSO_4$ as the reference sample.

Transient Absorption Experiments

Samples used for the laser flash photolysis experiments were prepared by adding an aqueous suspension of the solid solutions to a quartz cell (10×2 mm). The samples were excited with pulses from a Q-switch third-harmonic Nd:YAG laser (355 nm, 5 ns FWHM). Excitation pulse energies were ~10 mJ/pulse. Transient absorption kinetics was observed using a CW He–Ne laser as a probe. All decay kinetics were monitored by following the trapped charge carrier absorption at 670 nm.

Measurement of Isoelectric Point

ζ potential measurements on the rutile TiO_2 calcined at 710°C and TiO_2 (Degussa) were carried out on a Brookhaven Zeta Plus analyzer. The suspension fluid was a 1 mM aqueous solution of potassium nitrate. The concentration of catalyst in this suspension was 0.5 mg ml^{-1}. The pH value of the suspension was adjusted by the addition of 0.1 M nitric acid and 0.1 M potassium hydroxide solutions.

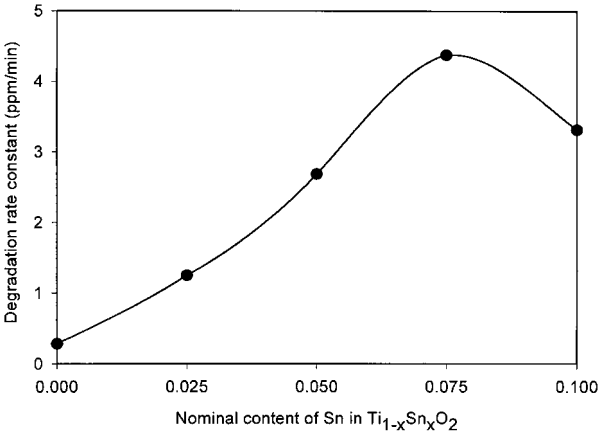

FIG. 1. Degradation rate constant of acetone over the surface of $Ti_{1-x}Sn_xO_2$ in rutile form as a function of Sn content.

RESULTS

Photocatalytic Activity

The rate constants for the degradation reaction of acetone over the solid solutions illuminated by UV light are shown in Fig. 1. The solid solutions of $Ti_{1-x}Sn_xO_2$ are shown to have much higher activity than pure rutile TiO_2 for the oxidation of acetone, and the activity increases with increasing Sn substitution for Ti in TiO_2 lattice. Noticeably, the activity begins to drop when the nominal $x = 0.10$.

Characterization Results

Analysis of phase constitution by XRD. From the polycrystalline X-ray diffraction patterns of the solid solutions $Ti_{1-x}Sn_xO_2$ ($0.00 \leq x \leq 0.10$) calcined at 710°C for 3 h (shown in Fig. 2), all samples are found to be rutile with

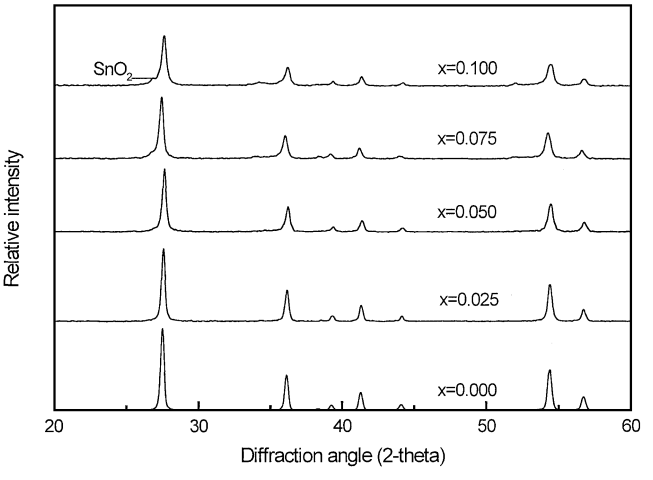

FIG. 2. Polycrystalline X-ray diffraction patterns of $Ti_{1-x}Sn_xO_2$.

the exception of sample $x = 0.10$, in which a small amount of SnO_2 is present; no anatase phase was detected in all samples.

Determination of lattice parameters and crystal size by XRD. To determine the lattice parameters of $Ti_{1-x}Sn_xO_2$ solid solutions in rutile, polycrystalline X-ray diffraction peaks of crystals (101) and (211), around which no diffraction peaks are present, were selected. The lattice parameters were obtained by using the equations

$$\text{(Bragg's law) } d_{(hkl)} = \lambda/2\sin\theta,$$

$$d^{-2}_{(hkl)} = h^2a^{-2} + k^2b^{-2} + l^2c^{-2},$$

where $d(hkl)$ is the distance between the crystal planes of (hkl); λ is the wavelength of X-ray used in the experiment; θ is the diffraction angle of the crystal plane (hkl); hkl is the crystal plane index; and a, b, and c are lattice parameters (in rutile form, $a = b \neq c$).

Crystal size was determined from diffraction peak (110) broadening with the equation

$$D = K\lambda/(\beta_c - \beta_s)\cos\theta,$$

where D is the crystal size of the solid solution; β_c and β_s are the FWHM of the sample and the standard, respectively; and λ and θ are the same as mentioned above.

Table 1 shows the lattice parameters, cell volume, and crystal size of $Ti_{1-x}Sn_xO_2$. It is very obvious that the lattice parameters and cell volume of the solid solutions increase with an increase in the level of Sn substitution for Ti in rutile TiO_2 lattice until the nominal $x = 0.075$, meaning that rutile TiO_2 is saturated with Sn at nominal $x = 0.075$. In sample $x = 0.10$, there is too much Sn to enter the TiO_2 lattice, and some Sn is present as SnO_2 as shown in Fig. 2. Table 1 also shows that the crystal size of the solid solutions decreases gradually with the addition of Sn to the TiO_2 lattice. The decrease in crystal size can be attributed to the presence of Sn–O–Ti in the solid solution which inhibits the growth of crystal grains.

Diffuse reflectance spectroscopy. Diffuse reflectance UV–vis spectra reveal that the absorption band (includes absorption edge and absorption maximum) of the solid solutions shifts gradually to shorter wavelengths with increasing Sn substitution for Ti in the TiO_2 lattice. The blue shift corresponds to an increase in bandgap.

TABLE 1

Lattice Parameters, Cell Volume, and Crystal Size of $Ti_{1-x}Sn_xO_2$

$Ti_{1-x}Sn_xO_2$	$a = b$ (Å)	c (Å)	Cell volume (Å^3)	Crystal size (nm)
$x = 0.00$	4.589	2.952	62.166	49.21
$x = 0.025$	4.589	2.952	62.166	45.20
$x = 0.05$	4.590	2.954	62.235	41.42
$x = 0.075$	4.595	2.968	62.666	36.27
$x = 0.10$	4.596	2.953	62.377	35.86

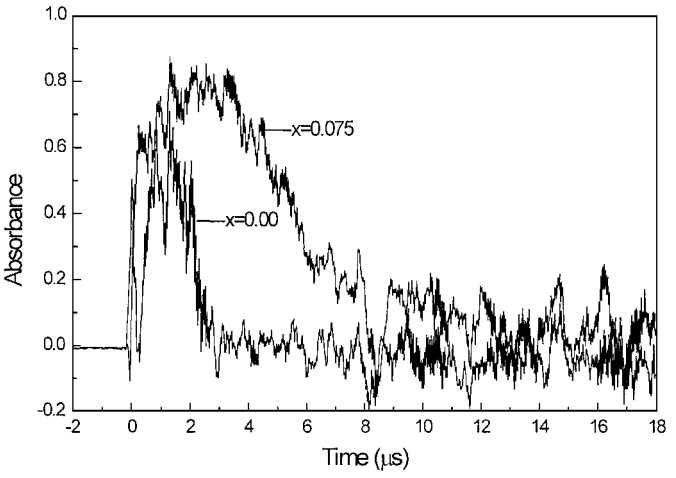

FIG. 3. Transient absorption decays observed at 670 nm on the microsecond scale.

Results of ζ Potential Measurements

The ζ potentials of rutile TiO_2 calcined at 710°C for 3 h and TiO_2 (P25 Degussa) were determined. According to the ζ potential values determined, they have isoelectric points at pH 4.71 and pH 5.25, respectively.

Results of Transient Absorption Measurements

From the decay profiles of photoexcited absorption shown in Fig. 3, it is very obvious that the solid solution $Ti_{1-x}Sn_xO_2$ ($x = 0.075$) has a much lower electron–hole recombination rate than rutile TiO_2.

DISCUSSION

Effects of Impurity Phase and Surface Hydroxyl Groups on Photoactivity

Based on the results of X-ray diffraction, the lattice parameters and cell volume of the solid solutions increase with increasing Sn substitution until $x = 0.075$, and all samples are composed of only rutile phase except for sample $x = 0.10$, in which a very small amount of SnO_2 is present. Of course, it is possible that some Sn is present as SnO_2 in other samples. Since the bandgap of the semiconductor SnO_2 is about 3.8 eV (19), its threshold wavelength, at which absorption is initiated, is about 326 nm. So, the wavelength of the light used in the photocatalytic experiment is not sufficient to promote electrons from its valence band to the conduction band. On the other hand, if electrons could be excited from the valence band to the conduction band, the electrons on the conduction band have no ability to reduce oxygen in air and would recombine rapidly with

photogenerated holes or hydroxyl radicals on the surface since the energy of the CB electron (defined in terms of the electrode potential vs NHE) is less negative than the standard redox potential of the O_2/O_2^- couple (E_{CB} for $SnO_2 = 0$ V vs NHE, and E_{NHE} for $O_2/O_2^- = -0.33$ V) (20). According to the above discussion, the presence of SnO_2 in solid solution samples is detrimental to photoactivity, which is elucidated by the photocatalytic performance of sample $x = 0.10$ with greater content of SnO_2, and is not responsible for the increase in photoactivity of the solid solutions.

Surface hydroxyl groups are thought to play an important role in determining photocatalytic activity, since these groups accept holes generated by UV illumination to form hydroxyl radicals and prevent electron–hole recombination (21, 22). Therefore, it is expected that a greater number of hydroxyl groups yield a higher reaction rate. Tsai and Cheng (16) also thought that the lower activity of rutile TiO_2 is due to the lack of hydroxyl groups on its surface. We also determined and compared the isoelectric points of a commercial anatase TiO_2 (P25) and our laboratory-made rutile TiO_2 calcined at 710°C. Interestingly, the results of ζ potential measurement show the rutile TiO_2 calcined at 710°C and TiO_2 (P25) have isoelectric points at pH 4.71 and pH 5.25, respectively. This means that there are more hydroxyl groups on the surface of rutile TiO_2 than on the surface of TiO_2 (P25), a widely used photocatalyst known for its high photoactivity. In other words, rutile TiO_2 has enough hydroxyl groups on its surface to trap photogenerated holes. The concentration of surface hydroxyl groups is not the most critical factor in determining photoactivity. As shown in Fig. 3, the electron–hole recombination rate is very fast on the rutile TiO_2 surface. Based on the experimental results for $Ti_{1-x}Zr_xO_2$ which we studied previously (23), Sn substitution for Ti in the TiO_2 lattice results in an increase in surface hydroxyl groups because the radius of Sn is larger than that of Ti. However, we cannot explain the increase in activity of the solid solution $Ti_{1-x}Sn_xO_2$ in rutile form by considering its concentration of surface hydroxyl groups.

Effects of Change in the Bandgap on Photoactivity

According to the above discussion, both impurity phase SnO_2 and surface hydroxyl groups are not responsible for the increase in photoactivity of the solid solutions. Diffuse reflectance UV–vis spectra reveal that the solid solutions show a blue shift in their absorption band as compared with rutile TiO_2. It has been suggested that a blue shift in absorption spectra could be an indication of a size-quantization effect (24, 25). Based on the following equation derived by Brus (26) from a particle in a sphere model for relating bandgap to particle radius,

$$\Delta E = \left(\frac{\hbar^2\pi^2}{2r^2}\frac{1}{\mu}\right) - \frac{1.8e^2}{r\varepsilon},$$

where r is the radius of the particle (crystal size), ε is the dielectric constant of the materials, and μ is the reduced mass of the excitation calculation from

$$\mu^{-1} = m_e^* + m_h^*,$$

where m_e^* is the mass of the electron and m_h^* is the mass of the hole.

Since the crystal size of solid solutions of $Ti_{1-x}Sn_xO_2$ is in the range 50–35 nm which is much larger than 10 nm, it is impossible that the increase in bandgap is the result of a quantum size effect. Therefore, the blue shift might result from the formation of new energy levels by the interaction of substituting Sn with the semiconductor lattice.

Transient absorption decay spectra show that the solid solution $Ti_{1-x}Sn_xO_2$ ($x = 0.075$) has a lower electron–hole recombination rate than rutile TiO_2. Since this result is in good agreement with the photocatalytic performance of the solid solutions for the oxidation of acetone in air, the solid solutions (including rutile TiO_2) should have the same photocatalytic performance in aqueous solution as in air. Therefore, we think it is reasonable to explain the photocatalytic activities of the samples by comparing the energy level of their conduction and valence bands with the reduction potential of O_2 in aqueous solution.

When rutile TiO_2 is irradiated by UV light of wavelength 365 nm, the UV absorption spectrum of rutile TiO_2 suggests that there is a strong absorption at about 365 nm. This means that a lot of electrons with potential larger than 2.8 V on the valence band are promoted to the conduction band. The holes (potential ≥ 2.8 V) left on the valence band are trapped by surface hydroxyl groups to form hydroxyl radicals. Those electrons on the conduction band are unable to reduce oxygen since the conduction band potential is about -0.30 V versus NHE (27), and the standard redox potential of the redox system O_2/O_2^- is $E^0_{NHE} = -0.33$ eV (20). These electrons on the conduction band are mobile and recombine with those hydroxyl radicals rapidly, as shown in Fig. 3.

Since a bandgap of a semiconductor is the difference between its conduction band and valence band, it is believed that the blue shift in the bandgap of the solid solutions $Ti_{1-x}Sn_xO_2$ is in large part due to an increase in its conduction band. When the solid solution is illuminated by UV light of wavelength 365 nm, the electrons with a potential of more than 2.8 V absorb these photons and are promoted to the conduction band. The holes that these electrons leave have more energy to oxidize the surface hydroxyl groups to form hydroxyl radicals as compared with those on the valence band of rutile TiO_2. Since the conduction band shifts toward higher potential, the energy of the electrons on the conduction band is enough to reduce oxygen in air. Thus, the photoexcited electrons and holes on the solid solution can be separated effectively and have a longer lifetime (see Fig. 3).

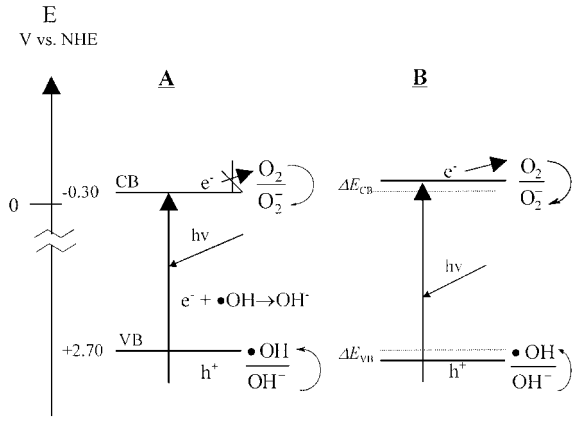

FIG. 4. Schematic diagram for the formation of charge carriers and the trapping of photogenerated electron and hole. (A) Rutile TiO_2; (B) Solid solution $Ti_{1-x}Sn_xO_2$ ($x = 0.075$).

From a thermodynamic point of view, the spontaneity of a photocatalytically induced redox reaction could be related to the position of the conduction and valence bands of the photocatalyst (28). The photocatalytic process system may also be considered an electrochemical cell, where the increase in bandgap results in an enhanced oxidation–reduction potential based on the equation

$$\Delta G = -zFE,$$

where E represents the bandgap of the semiconductor, ΔG is the free energy change of the redox process occurring in the system, z is a positive integer equal to the number of elementary charges involved in the redox process, and F is the Faraday constant. Since the photogenerated electron–hole pairs are effectively separated in the $Ti_{1-x}Sn_xO_2$ solid solutions, these photocatalysts have a lower electron–hole recombination rate as compared with rutile TiO_2. Figure 4 is a schematic diagram for the formation of charge carriers and the trapping of photogenerated electrons and holes.

CONCLUSIONS

Sn^{4+} substitution for Ti^{4+} in the rutile TiO_2 lattice results in a decrease in the rate of photogenerated electron–hole recombination. This lower recombination rate can be related to an increase in the bandgap of the solid solution. The elevation of the semiconductor's bandgap causes an increase in its photocatalytic oxidation–reduction potential, which is the origin of the enhanced photoactivity of $Ti_{1-x}Sn_xO_2$.

ACKNOWLEDGMENT

The work described in this paper was partially supported by a grant from the Research Grants Council of the Hong Kong Special Administrative Region, China (RGC Ref. No. CUHK4124/98P).

REFERENCES

1. Ollis, D. F., and Al-Ekabi, H. (Eds.), "Photocatalytic Purification and Treatment of Water and Air." Elsevier, Amsterdam, 1993.
2. Carraway, E. R., Hoffman, A. J., and Hoffmann, M. R., *Environ. Sci. Technol.* **28**, 786 (1994).
3. Rao, M. V., Rajeshwar, K., Verneker, V. R. Pai., and DuBow, J., *J. Phys. Chem.* **84**, 1987 (1980).
4. Nishimoto, S., Ohtani, B., Kajiwara, H., and Kagiya, T., *J. Chem. Soc. Faraday Trans.* **81**, 61 (1985).
5. Ohko, Y., Fujishima, A., and Hashimoto, K., *J. Phys. Chem. B* **102**, 1724 (1998).
6. Hoffmann, M. R., Martin, S. T., Choi, W., and Bahnemann, D. W., *Chem. Rev.* **95**, 69 (1995).
7. Muggli, D. S., Larson, S. A., and Falconer, J. L., *J. Phys. Chem.* **100**, 15886 (1996).
8. Nishida, S. Y., Fu, X., Anderson, M. A., and Hori, K., *J. Photochem. Photobiol. A* **97**, 175 (1996).
9. Rekoske, J. E., and Barteau, M. A., *J. Catal.* **165**, 57 (1997).
10. Peterson, M. W., Tuner, J. A., and Nozik, A. J., *J. Phys. Chem.* **95**, 221 (1991).
11. Martin, S. T., Morrison, C. L., and Hoffmann, M. R., *J. Phys. Chem.* **98**, 13695 (1994).
12. Choi, W., Termin, A., and Hoffmann, M. R., *J. Phys. Chem.* **98**, 13669 (1994).
13. Hoffmann, A. J., Carraway, E. R., and Hoffmann, M. R., *Environ. Sci. Technol.* **28**, 776 (1994).
14. Takeda, N., Iwata, N., Torimoto, T., and Yoneyama, H., *J. Catal.* **177**, 240 (1998).
15. Sampath, S., Uchida, H., and Yoneyama, H., *J. Catal.* **149**, 189 (1994).
16. Tsai, S. J., and Cheng, S., *Catal. Today* **33**, 227 (1997).
17. Sclafani, A., Palmisano, L., and Schiavello, M., *J. Phys. Chem.* **94**, 829 (1990).
18. Maruska, H. P., and Ghosh, A. K., *Sol. Energ.* **20**, 443 (1978).
19. Vinodgopal, K., and Kamat, P. V., *Environ. Sci. Technol.* **29**, 841 (1995).
20. Bard, A. J., Parsons, R., and Jordan, J. (Eds.), "Standard Potentials in Aqueous Solution." Marcel Dekker, New York, 1985.
21. Fu, X., Clark, L. A., Yang, Q., and Anderson, M. A., *Environ. Sci. Technol.* **30**, 647 (1995).
22. Do, Y. R., Lee, W., Dwight, K., and Wold, A., *J. Solid State Chem.* **108**, 198 (1994).
23. Yu, J. C., Lin, J., and Kwok, R. W. M., *J. Phys. Chem. B* **102**, 5094 (1998).
24. Anderson, C., and Bard, A. J., *J. Phys. Chem. B* **101**, 2611 (1997).
25. Anpo, M., Shima, T., Kodama, S., and Kubokawa., *J. Phys. Chem.* **91**, 4305 (1987).
26. Brus, L. E., *J. Chem. Phys.* **79**, 5566 (1983).
27. Serpone, N., and Pelizzetti, E. (Eds.), "Photocatalysis Fundamentals and Applications." Wiley, New York, 1989.
28. Palmisano, L., and Sclafani, A., *in* "Heterogeneous Photocatalysis" (M. Schiavello, Ed.), p. 109, Wiley, New York, 1997.